

## Feature Article

# Studies on Self-Assembled Alkanethiol Monolayers Formed at Applied Potential on Polycrystalline Gold Electrodes

Christopher M. A. Brett,<sup>\*a</sup> Slavoj Kresak,<sup>a,b</sup> Tibor Hianik,<sup>b</sup> Ana Maria Oliveira Brett<sup>a</sup>

<sup>a</sup> Departamento de Química, Universidade de Coimbra, 3004-535 Coimbra, Portugal

\* e-mail: brett@ci.uc.pt

<sup>b</sup> Department of Biophysics and Chemical Physics, Comenius University, Mlynská dol. F1, 84248 Bratislava, Slovakia

Received: July 27, 2002

Final version: October 14, 2002

## Abstract

1-Dodecanethiol assembly on polycrystalline gold electrodes at fixed positive potentials has been investigated by chronoamperometry and electrochemical quartz crystal microbalance and the films formed characterized by cyclic voltammetry and electrochemical impedance spectroscopy. It was found that 1-dodecanethiol adsorption on gold is enhanced by application of positive potentials to the electrode surface and that adsorption proceeds faster than in the case of open circuit deposition. Compact defect-free monolayers of capacitance values of 1.1–1.6  $\mu\text{F cm}^{-2}$  are produced in time intervals as short as 100 s, with no roughness, as demonstrated for the first time by electrochemical impedance analysis. Control of surface potential during alkanethiol assembly appears to improve monolayer quality and to allow for shorter assembly periods. Monolayers can be removed by cycling in alkaline solution or in dilute sulfuric acid. These results are important for the fast construction of defect-free bilayers.

**Keywords:** Self-assembled monolayers, Cyclic voltammetry, Electrochemical impedance spectroscopy

## 1. Introduction

Spontaneous adsorption of organic molecules from solution onto solid surfaces can give rise to self-assembled monolayers (SAMs). Alkanethiols ( $\text{CH}_3(\text{CH}_2)_n\text{SH}$ ) and related molecules spontaneously adsorb onto noble metals, particularly gold, to form close-packed oriented SAMs [1–3]. The affinity of the sulfur for the metal and the strength of the bond formed, predominantly covalent with some polar character, are significant [4, 5]. The adsorbate head group-substrate bonds, the lateral van der Waals interactions between the molecules and the density of packing result in sufficient stability that the monolayer resists removal by solvent rinsing. The self-assembly method does not require anaerobic or anhydrous conditions. SAMs also provide a means of attaching to the electrode a diverse set of structures ranging from modified monolayers to multilayers, e.g., [6, 7].

SAMs provide a means of defining the chemical composition and structure of a surface, and because of this have become the focus of intensive investigation. It is possible to attach a wide range of functional groups as head groups to the adsorbing molecule without disrupting the self-assembly process or destabilising the SAM. Thus, a variety of modified alkanethiols have been used successfully to coat metal surfaces with SAMs with unique properties. If such a modified SAM is uniform in composition and densely packed, then a single functional group is exposed on the external surface. This property permits the exploitation of the effect of surface composition on surface-sensitive properties such as wetting, friction and adhesion [8].

Sulfur-based SAMs also seem to be promising in corrosion prevention [9], sensors and biosensors [10–12], electrocatalysis [13] and preparation of micropatterned surfaces that might find their use in nanoscale lithography [14]. A better understanding of the factors controlling electron transfer over long distances and under large driving forces can also be gained [15].

The normal method for making SAMs is to allow the process to occur spontaneously at open circuit. Evidence is that adsorption occurs quickly followed by a slow reorganization of the adsorbed layer over a period of many hours [16, 17]. Applying a positive potential can alter the characteristics of the monolayers formed and increase the kinetics of formation [18–21]. It is our purpose to make bilayer lipid membranes and there are very useful effects to be gained from making the first alkanethiol layer fast. The efficiency of desorption of the monolayers in alkaline solution at negative potentials has also been investigated [22, 23].

In this article, the self assembly of 1-dodecanethiol on polycrystalline gold electrodes at fixed positive applied potentials has been investigated in detail. Cyclic voltammetry was utilized to examine the degree of order and compactness of the monolayers formed. Monolayer capacitance was determined by means of electrochemical impedance spectroscopy; and gave information on the effective roughness of the SAM. Chronoamperometry, chronopotentiometry and the quartz crystal microbalance were also used to examine the rate of assembly.

## 2. Experimental

### 2.1. Apparatus and Reagents

Smooth silicon plates of rectangular shape, approximately  $4 \times 10$  mm, 1 mm thick, with a thin layer of sputtered gold on one side, were used as substrates for dodecanethiol monolayer assembly. The gold layer comprised 2 distinct areas, a working area of a) circular (0.7 mm in diameter) or b) square ( $1.5 \times 1.5$  mm) shape, external contact being made through a thin gold strip.

The cell used throughout the electrochemical experiments was a ca. 3 mL mini/micro electrode glass cell. An Ag/AgCl/saturated KCl electrode was used as reference in all experiments. A clean Pt wire or foil of rectangular shape was used as a counter electrode in aqueous solutions, and was substituted for a glassy carbon electrode in ethanolic solutions.

Cyclic voltammetry, chronoamperometry and open circuit potential measurements were performed using either an EG&G PAR 273A, or an Eco-Chemie  $\mu$ Autolab Type II potentiostat/galvanostat with computer control. Electrochemical impedance spectroscopy measurements were performed using a Solartron 1250 Frequency Response Analyser with 1286 Electrochemical Interface, controlled with ZPLOT Electrochemical Impedance Software; data analysis was carried out using the ZSIM/CNLS Impedance Simulation and Modelling Software. A 10 mV rms amplitude voltage perturbation was applied in the frequency range 65 kHz down to 0.1 Hz, with 10 points per frequency decade.

Electrochemical quartz crystal microbalance (EQCM) experiments were performed on 10 MHz AT-cut quartz crystals, plated on both sides with gold. The crystals were mounted in a homemade EQCM cell, connected to an oscillator circuit, a Hewlett Packard 53131A Universal Counter and an EG&G PAR 273A potentiostat. The gold-plated area of the crystal exposed to the solution was used as the working electrode. The same counter and reference electrodes were used as for the electrochemical experiments.

1-Dodecanethiol was obtained from Sigma. All solutions were made with analytical grade reagents and ultrapure water (Milli-Q<sup>50</sup>, Millipore) or absolute ethanol (99.8%, Merck). Phosphate buffer, 0.1 M pH 7.4, was the main supporting electrolyte employed in aqueous solution; sodium perchlorate was used in ethanolic solutions. Potassium ferrocyanide was utilized to test the cleanliness of gold surfaces and the blocking behavior of assembled monolayers. Sodium hydroxide and dilute sulfuric acid were used in cleaning procedures.

### 2.2. Electrochemical Cleaning Procedure

In accordance with previous findings concerning alkanethiol desorption [22, 23], linear sweep voltammetry in 0.5 M NaOH was utilized to remove SAMs from electrodes. The

potential was swept from 0 to  $-1.5$  V at 0.1 V per second, followed by a 30–60 second potential pause at ca.  $-1.4$  V, this value of potential being sufficiently negative to cause desorption of a 1-dodecanethiol monolayer from gold.

Electrochemical cycling into the gold oxide formation region in dilute acid was employed after cathodic stripping or as another cleaning and annealing process. Gold electrodes were cycled in 0.1 M H<sub>2</sub>SO<sub>4</sub> between  $-0.4$  V and  $+1.7$  V (vs. Ag/AgCl saturated KCl) at 0.1 V s<sup>-1</sup> scan rate. The surface was considered clean upon reaching a cyclic voltammetry curve with stable gold oxide formation and reduction peaks, invariant between successive cycles. To avoid any possible readsorption of desorbed dodecanethiol, the working electrode was rinsed in water and transferred into a second, fresh sulfuric acid solution for additional cycling.

During preliminary studies, chemical oxidation of gold by means of “piranha” solution was used to obtain clean surfaces, accomplished by immersion for ca. 3 minutes. This was abandoned during the course of the work since it was found to be too harsh a treatment for the evaporated gold films.

### 2.3. Experimental Monolayer Assembly Procedure

In a typical procedure, a gold-covered silicon plate or quartz crystal was first cleaned in sulfuric acid and rinsed with water and ethanol. 1-Dodecanethiol monolayer assembly was then carried out. This was carried out in two ways:

a) After a period of 300–500 s for stabilization of the clean working electrode in 0.1 M NaClO<sub>4</sub> in ethanol, at the chosen applied potential or at open circuit, an aliquot of 1-dodecanethiol in 0.1 M NaClO<sub>4</sub> was then added to obtain a final concentration of 1 mM.

b) All components were mixed prior to immersion of the electrode in the solution, to ensure a constant concentration of 1 mM 1-dodecanethiol throughout the whole assembly period.

After assembly, the electrode with its gold surface now partially or completely covered with 1-dodecanethiol, was again rinsed thoroughly in both solvents, this time in reverse order. It was then transferred promptly to phosphate buffer and allowed to stabilize for 10 min. Cyclic voltammetry, was then carried out until smooth and stable voltammograms were obtained. Following this, the electrode was normally exposed to ambient atmosphere to certify that the transfer to the electrochemical impedance apparatus, requiring approximately a 60 s exposure of the working electrode to air, would not change the nature of the assembled layer. After checking the voltammogram upon reimmersion, the actual transfer to the EIS equipment took place and impedance measurements were performed. Subsequently, another cyclic voltammogram was recorded. Next, the electrode was rinsed with water and transferred to the solution of phosphate buffer with potassium ferrocyanide to check film integrity. The process of cyclic voltammetry and impedance measurements in electrolyte was then repeated

to ensure that no changes to the monolayer had occurred. Finally, the electrode was placed in 0.5 M NaOH where reductive desorption of 1-dodecanethiol monolayer from gold was performed. After electrochemical cleaning in sulfuric acid, the electrode was ready for another 1-dodecanethiol assembly process.

### 3. Results and Discussion

#### 3.1. Formation of SAMs

The useful values of potential for carrying out 1-dodecanethiol monolayer assembly were determined by cyclic voltammetry in ethanolic and also in aqueous 0.1 M NaClO<sub>4</sub>, since “absolute” ethanol contains a small percentage of water that might play an important role in alkanethiol adsorption above the oxidation potential of gold, see Figure 1. Selected potentials (0.6, 0.9, 1.2 and 1.5 V vs. Ag/AgCl) include a value of +0.9 V that is located just below the potential of the onset of gold oxide formation, and values in regions where gold oxidation (above +0.9 V) and ethanol oxidation (above +0.6 V [24]) oxidation occurs.

SAMs formation was followed by chronoamperometry. Figure 2 gives examples of the general response of gold electrodes held at fixed positive potentials to the addition of 1-dodecanethiol. Variations in peak shapes and amplitudes observed for different experiments performed at identical potentials can be ascribed to changes in the adsorption process due to differences in the surface morphology and structure.

For potentials of 0.6 V and 0.9 V, addition of 1-dodecanethiol to the ethanolic solution is followed immediately by an anodic current that rises and declines back to zero over less than 150 s, with a maximum value of about 100  $\mu\text{A cm}^{-2}$ . The anodic process can be represented by [4, 25]



The fact that an anodic current occurs suggests that the alternative mechanism with formation of molecular hydrogen [3], if it does take place, cannot account for all the monolayer formation.

At 1.2 V and 1.5 V, a significant constant faradaic current flowed through the circuit prior to addition, owing to oxidation of ethanol and water at the electrode surface. On adding 1-dodecanethiol, peaks very similar to those obtained at lower potentials appeared, but falling nearly to zero instead of to their initial constant levels. This can be explained by the fact that, upon coating, the redox processes taking place continue only where there are pinholes and defects in the covering layer [19].

An estimation of the charge that flowed through the circuit in response to addition of 1-dodecanethiol in the system can be obtained by integration of the chronoamperometric curve with respect to time, as suggested previously [21]. Assuming one elementary charge is associated with each adsorbed 1-dodecanethiol molecule, the number

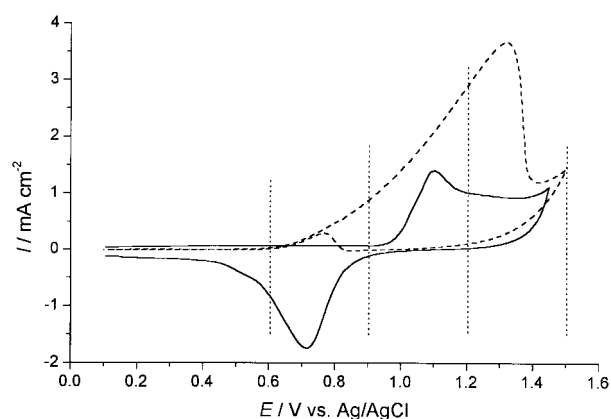


Fig. 1. Cyclic voltammograms of gold electrodes recorded in (—) aqueous and (---) ethanolic (99.8%) 0.1 M NaClO<sub>4</sub> solutions at 100 mV s<sup>-1</sup> scan rate. Dotted vertical lines represent the values of potentials to be applied to gold working electrodes during the process of 1-dodecanethiol monolayer assembly.

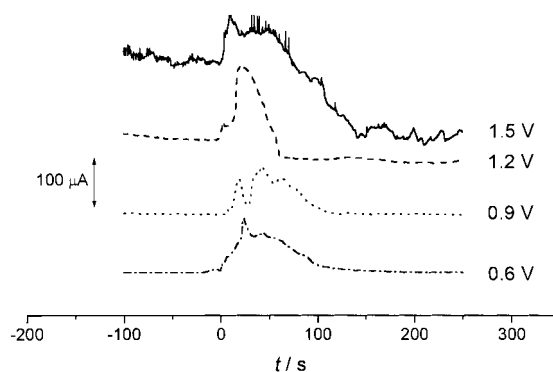


Fig. 2. Chronoamperometric traces following 1-dodecanethiol monolayer assembly from 0.1 M NaClO<sub>4</sub> + 1 mM 1-dodecanethiol in ethanol at various fixed potentials. 1-Dodecanethiol was added at  $t = 0$ .

of 1-dodecanethiol molecules on the surface per unit area considering the tightest packing density of alkanethiols on regular smooth Au(111) [26], namely 0.214 nm<sup>2</sup> per thiol or  $4.673 \times 10^{14}$  thiol per cm<sup>2</sup>, a charge of 74.9  $\mu\text{C cm}^{-2}$  would be expected on formation of a complete alkanethiol monolayer. Surprisingly, integration of chronoamperometric curves obtained in our experiments yields values of 7.8 to 8.4 mC cm<sup>-2</sup>, about two orders of magnitude higher than expected. Although there could be multilayer formation [7], there are other possible explanations. One is the oxidation of thiols to disulfides with formation of protons, which consumes charge. After formation the disulfides are released into solution. A second contribution to the measured charge could arise from enhanced ethanol oxidation accompanying adsorption.

Open circuit potential adsorption is shown in Figure 3. Addition of 1-dodecanethiol into the ethanolic supporting electrolyte repeatedly caused an abrupt negative change in the OCP of the gold electrode. A short time lag between

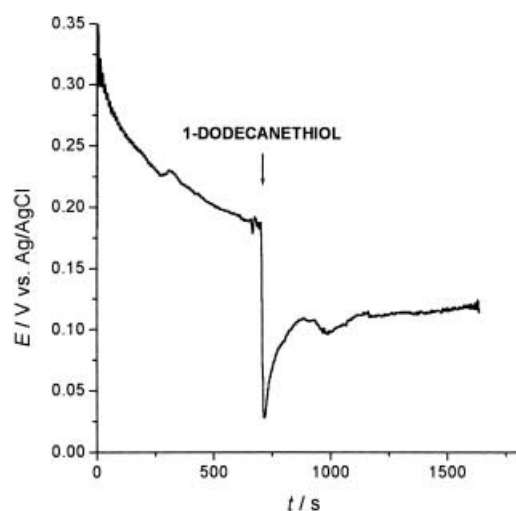


Fig. 3. Representative open circuit potential vs. time response of gold to addition of 1-dodecanethiol to ethanolic 0.1 M NaClO<sub>4</sub>, to final concentration of 1 mM.

addition and potential drop appeared owing to the limited rate of diffusion of 1-dodecanethiol molecules to the electrode surface. There followed a gradual increase to a value between the minimum and that prior to 1-dodecanethiol addition. The reasons for such a negative peak occurrence are currently unknown. Nevertheless, the change in OCP in the negative direction implies electron transfer from the thiol molecules into the metal film [21], and is thus in agreement with the data obtained at fixed applied potential.

### 3.2. Voltammetric Characterization of SAMs Compared to Clean Gold Surfaces

It was important to ensure that electrode surfaces were not altered by the deposition procedure itself. Therefore, control experiments during which the complete procedure of 1-dodecanethiol assembly was simulated in the absence of 1-dodecanethiol were performed and the ferro/ferricyanide redox couple was used to probe the surface activity of gold electrodes. Figure 4a shows cyclic voltammograms in phosphate buffer + 1 mM K<sub>4</sub>[Fe(CN)<sub>6</sub>] of two clean gold electrodes both of which were immersed in the ethanolic sodium perchlorate solution (supporting electrolyte used for all 1-dodecanethiol assembly experiments) for 300 s, one at open circuit and the other at an applied potential of +0.6 V. The voltammograms are essentially equal, so that it can be assumed that the nature of the surface after both treatments is identical. Similar blank treatments at different potentials yielded equivalent voltammetric characteristics as depicted in the figure.

Figure 4b shows cyclic voltammograms obtained under the two same conditions as above, except for the presence of 1-dodecanethiol in the ethanolic sodium perchlorate at the concentration of 1 mM. The voltammogram of the electrode immersed in the 1-dodecanethiol solution at OCP exhibits

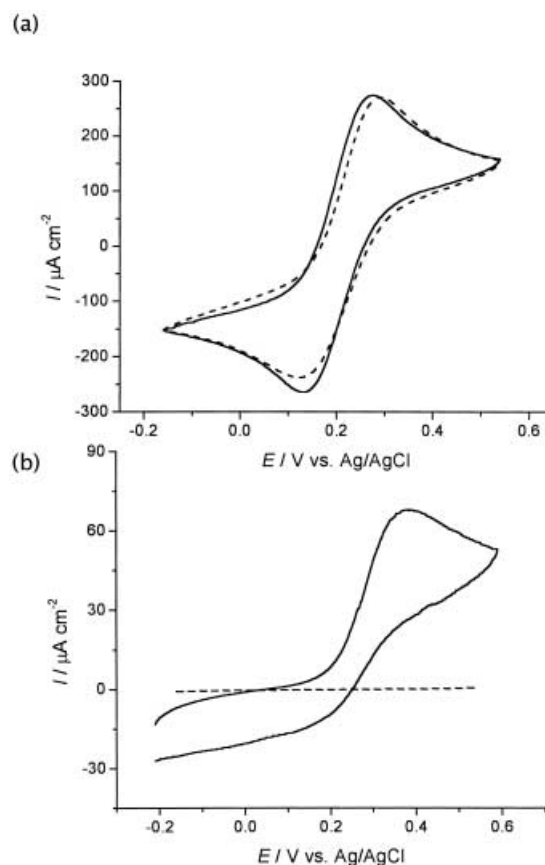


Fig. 4. Cyclic voltammograms (scan rate 50 mV s<sup>-1</sup>) in 0.1 M pH 7.4 phosphate buffer + 1 mM K<sub>4</sub>[Fe(CN)<sub>6</sub>] of two clean gold electrodes immersed for 300 s in a) ethanolic 0.1 M NaClO<sub>4</sub> electrolyte, b) ethanolic 0.1 M NaClO<sub>4</sub> electrolyte + 1 mM 1-dodecanethiol. Solid line, open circuit potential; dashed line, 0.6 V vs. Ag/AgCl.

the character of a quasi-reversible system. The occurrence of the oxidation peak and the reduction “wave” after this immersion time are indicative of pinholes on the surface where electron transfer between the electroactive ion and the metal surface can proceed and that the film is of rather poor integrity. On the other hand, the voltammogram of the electrode with monolayer assembled at 0.6 V (dashed curve) does not exhibit any oxidation or reduction peak, suggesting the absence of major pinholes and vacancy spots in the monolayer. This is further evidence that full monolayer 1-dodecanethiol assembly on a gold surface at 0.6 V proceeds at a significantly higher rate with potential control.

Equivalent experiments carried out at different assembly potentials gave the same results: the voltammograms of SAMs formed at potentials in the range 0.6 to 1.5 V are very similar and no trace of electron transfer processes can be observed.

### 3.3. Electrochemical SAM Removal and Cleaning of Gold Substrates

Linear sweep voltammetry in 0.5 M NaOH was utilized to remove SAMs from electrodes. Alkaline environments have

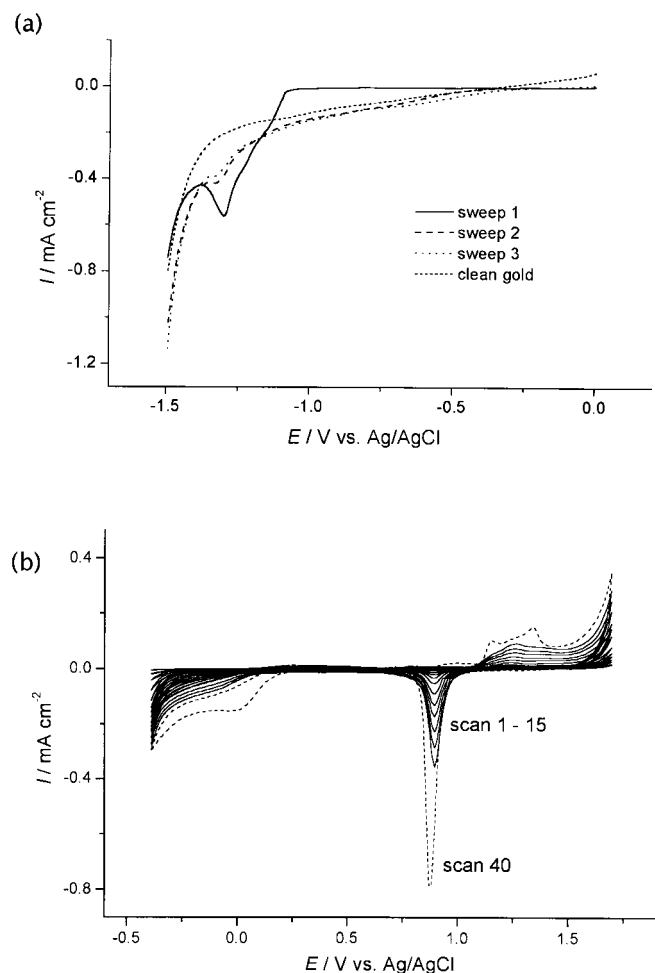


Fig. 5. a) Cyclic voltammograms in 0.5 M NaOH showing cathodic desorption of a 1-dodecanethiol monolayer previously formed at 0.6 V during 300 s. Three successive cycles (1, 2, and 3, respectively), only the sweeps in the negative direction are shown. Scan rate 50 mV s<sup>-1</sup>. b) Electrochemical voltammetric cycling of monolayer-covered gold in 0.1 M H<sub>2</sub>SO<sub>4</sub>, 40 scans. Scan rate 50 mV s<sup>-1</sup>.

been previously used for this purpose [22, 23, 27, 28]. Figure 5 is an example of reductive desorption of a 1-dodecanethiol monolayer from the gold surface. In sweep 1 a current begins to flow at -1.1 V with a cathodic peak at -1.3 V due to monolayer desorption and consequent capacitive current. Sweeps 2 and 3 both bear a trace of the desorption peak, ascribable to desorption of thiol that might have readsorbed to gold when the potential was above -1.1 V.

Figure 5b shows an alternative, although slower, to stripping of 1-dodecanethiol monolayers in alkaline environment but which could represent a very useful and easier cleaning method. This involves repeated voltammetric cycling between hydrogen and oxygen evolution regions in dilute sulfuric acid. Since initially the surface is coated with almost a complete monolayer, the currents obtained in the first scans are very low. The increase continues until all the electrode surface is free of contaminants and exposed to

solution. Scan 40 represents a typical voltammogram of a clean polycrystalline gold surface.

### 3.4. Electrochemical Impedance Spectroscopy

Electrochemical impedance spectra of clean gold surfaces and of monolayers were acquired. Previous recent studies in the literature using electrochemical impedance have concentrated on monitoring adsorption kinetics [16, 18], characterization of defects and possibility of any electron transfer through the monolayer film [29, 30]. Our results to be described below show that, under the formation conditions employed, there is no evidence of defects in the monolayer or electron transfer through it.

All complex plane plots consisted of straight lines with an angle of 90° or less than 90° which can be modelled by a capacitance with constant phase angle (*CPE*) characteristics, in series with the cell resistance. The *CPE* represents the surface roughness, which for a capacitance is characterized by an admittance  $k(i\omega)^\alpha$ , where  $k$  is a constant,  $\omega$  is the angular frequency,  $i$  is the imaginary unit, and the exponent  $\alpha$  varies from 1, for a smooth surface, to 0.5 for a porous electrode [31]. The Bode plots in Figure 6 give examples of impedance spectra of a 1-dodecanethiol monolayer formed on gold at 0.9 V (vs. Ag/AgCl/saturated KCl) in 1000 s, with those of clean gold and from a monolayer formed at open circuit potential, for comparison.

As can be observed, spectra of monolayers have noticeably larger impedance magnitude, due to a reduction of interfacial capacitance: the relative dielectric constant is reduced greatly as water molecules are excluded from the interface by an organic layer. The spectra of the two monolayers, one having been assembled at OCP during 14 hours and the other at a fixed positive potential during 1000 s, are almost identical, suggesting only minute differences in the monolayer capacitances that are a close reflection of their structure.

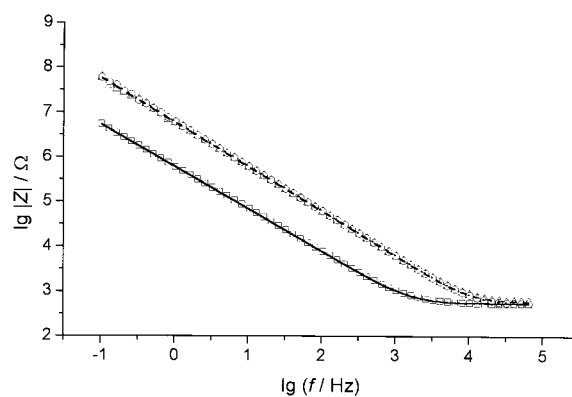


Fig. 6. Impedance magnitude Bode plots of spectra of clean gold ( $\square$ ) and of 1-dodecanethiol monolayers formed at a fixed potential of 0.9 V vs. Ag/AgCl during 1000 s ( $\triangle$ ) and at open circuit potential during 14 h ( $\circ$ ). The fitting of spectra is shown by the solid lines.

Table 1. Capacitance,  $C$ , resistance,  $R$ , and  $\alpha$  parameter values obtained from impedance spectra of clean gold and 1-dodecanethiol monolayer in Figure 7.

	$C$ ( $\mu\text{F cm}^{-2}$ )	$R$ ( $\Omega \text{ cm}^2$ )	$\alpha$
Clean gold	12.4	12.4	0.85
Monolayer formed at 0.9 V	1.17	13.5	1.0
Monolayer formed at OCP	1.14	12.4	1.0

Table 2. Capacitance values of 1-dodecanethiol monolayers assembled on gold at fixed positive potentials over 90, 300 and 1000 s intervals. All values are given in  $\mu\text{F cm}^{-2}$ .

Applied potential	Assembly time (s)		
	90	300	1000
0.3 V	–	2.65	–
0.6 V	1.51	1.12	1.38
0.9 V	1.08	1.67	1.58
1.2 V	1.43	1.52	1.24
1.5 V	1.58	1.79	–

The  $R + CPE$  circuit parameters from fitting of the data shown in Figure 6 are listed in Table 1. The capacitance of the monolayers is one order of magnitude smaller than that of the gold-buffer interface prior to monolayer formation, in agreement with other findings [32].

While 1-dodecanethiol monolayer assembly does not change the cell resistance, it has a strong effect on  $\alpha$ , the  $CPE$  exponent. The clean gold-buffer interface is best adjusted with an  $\alpha$  parameter of 0.85, indicative of a certain roughness of the solid gold surface. In contrast, forming the monolayer following either of the experimental procedures leads to  $\alpha$  values of unity, suggesting a monolayer-covered interface has the characteristics of an ideal capacitor. This important result shows that the 12-carbon-long hydrocarbon chains of 1-dodecanethiol, which are aligned parallel to each other and protruding from the metal into the electrolyte form a hydrophobic region that is able to compensate for the surface roughness of the gold surface.

A possible explanation is as follows. It is probably rather unfavorable energetically for the alkanethiol tips to locally stick out from the hydrophobic into the aqueous region of the monolayer-buffer interface, or to form small holes in the surface as would be expected if the monolayer surface followed the irregularities of the substrate. Thus, should a bump occur on the gold surface, the hydrocarbon chains that directly cover it and those that surround it are likely to constrict and stretch, respectively, to accommodate for the irregularity. An indentation would be compensated for analogously in the inverse fashion. This would lead to an essentially smooth monolayer surface as implied by the  $\alpha$  parameter values obtained from analysis of the impedance spectra.

Table 2 gives values of capacitance per unit area from analysis of 1-dodecanethiol monolayers formed at different potentials. Most of the resulting values fall in the range 1.1 –

1.6  $\mu\text{F cm}^{-2}$  as found in other work [16, 32]. Interestingly, within the range of potential and assembly time investigated, the monolayer capacitance seems not to depend either on the value of applied potential or on the assembly time.

Assembly at open circuit potential over a period of 15 h led to a final capacitance of 1.45  $\mu\text{F cm}^{-2}$  (52  $\mu\text{F cm}^{-2}$  after 300 s adsorption). Comparison with Table 2 shows that the final capacitances are essentially the same.

In all cases, the  $CPE$  exponent was close to unity after SAM formation, showing the ability of the SAM to compensate for the effective surface roughness of the gold substrate.

### 3.5. Electrochemical Quartz Crystal Microbalance

The response of the resonant frequency of clean gold-covered quartz crystals to variation of potential in phosphate buffer, pH 7.4 and aqueous 0.1 M  $\text{NaClO}_4$  (Figure 7a),

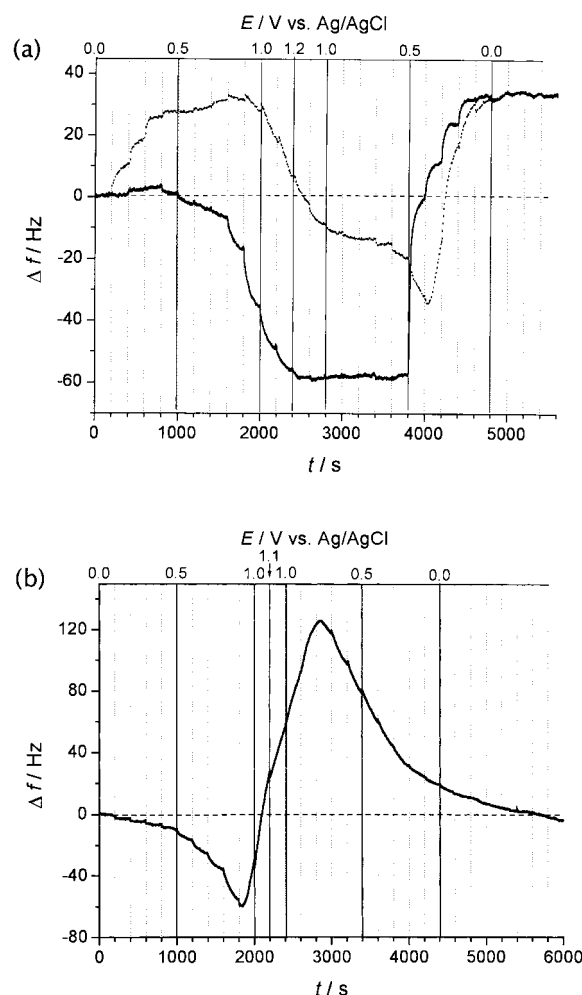


Fig. 7. Quartz crystal resonant frequency change with respect to potential in a) aqueous solutions of 0.1 M phosphate buffer, pH 7.4 (solid line), and 0.1 M  $\text{NaClO}_4$ , pH 5.4 (dotted line). b) ethanolic  $\text{NaClO}_4$ , 0.1 M. The potential is stepped 100 mV each 200 s; after reaching 0 V again the system is held at a constant potential of 0.0 V.

and ethanolic 0.1 M NaClO<sub>4</sub> (Figure 7b) were tested, stepping the potential by 100 mV increments every 200 s. Different responses are obtained.

In phosphate buffer the frequency change above 0.8 V is attributable to gold oxide formation with consequent mass increase. The rate of frequency decrease diminishes as the gold surface becomes completely covered with oxide. On the inverse scan, at 0.5 V gold oxide reduction begins, accompanied by an immediate and rapid frequency rise. The final level at 0.1 V ( $t = 4800$  s) is about 30 Hz higher than the initial value, suggesting some detachment of gold from the crystal due to gold oxide formation and reduction. This effect was reproducible.

In aqueous 0.1 M NaClO<sub>4</sub> the frequency changes in a different manner, starting with an increase from 0 to 0.3 V. A larger fall in frequency as a result of gold oxidation occurred in the interval of 0.9 to 1.2 V and continues of inverting the potential change. Another abrupt frequency fall could be observed at 0.5 V, followed by a sharp rise at 0.4 V as a consequence of oxide reduction. Similarly to phosphate buffer, the resonant frequency ended above that at the beginning of the experiment. Oxidation and reduction in sodium perchlorate solution took place at higher potentials owing to the lower pH of this solution in comparison to phosphate buffer. A possible explanation of these phenomena relates to changes of frictional forces at the solution-crystal interface as a function of surface potential: stepping the potential in either direction will lead to rearrangements of ions in the interfacial double-layer.

In ethanolic sodium perchlorate, the supporting electrolyte for 1-dodecanethiol adsorption, a different course of resonant frequency response to surface potential was observed (Figure 7b). Unlike the aqueous equivalent, the resonant frequency curve exhibits a negative slope as the potential is increased from 0 V. Above 0.9 V, there is a sharp frequency increase. Such behavior cannot be explained simply in terms of mass decrease. Examining the curve it can be seen that after restoring the initial potential of 0.0 V the frequency is close to its initial value, suggesting that removal of gold from the crystal has not occurred. It is known, however, that at potentials such as 0.9 V oxidation of ethanol to acetaldehyde starts to take place, and that a redox reaction between gold oxide and ethanol can occur [19, 24], also leading to production of acetaldehyde. Similar effects have been observed with oxides on passivated nickel and iron electrodes [33]. As acetaldehyde is produced at the gold surface the volume fraction of acetaldehyde and ethanol at the gold surface will grow and decline, respectively. A comparison of dynamic viscosity values for the two fluids at 20 °C (1.2 mPa s for ethanol, 0.22 mPa s for acetaldehyde [34]) shows acetaldehyde is 6 times less viscous than ethanol. With the increasing fraction of acetaldehyde, the viscosity of the mixture at the surface will fall, and so will the friction at the crystal-solution interface leading to a rise of the crystal resonant frequency [35]. Below 0.8 V (2800 s) the resonant frequency begins to decline again, i.e., below the potential necessary for ethanol oxidation.

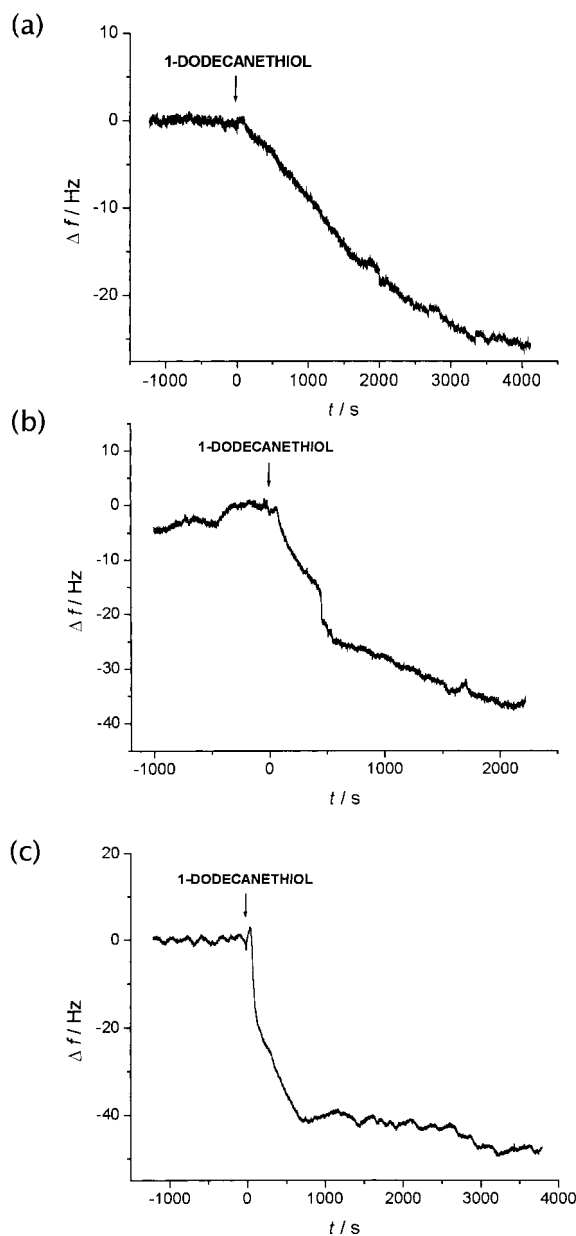


Fig. 8. Quartz crystal resonant frequency change after addition of 1-dodecanethiol to ethanolic 0.1 M NaClO<sub>4</sub> to final concentration of 1 mM at a) open circuit potential b) 0.0 V vs. Ag/AgCl and c) 0.6 V vs. Ag/AgCl.

Monitoring of resonant frequency change of the gold plated QCM related to 1-dodecanethiol adsorption was performed at 0.0, 0.6 and 1.2 V, as well as at the open circuit potential. Figures 8 and 9 show the results of experiments done under different conditions. In Figure 8 are results obtained at open circuit potential, and at applied potentials of 0.0 V and of 0.6 V. In Figure 9 is shown the QCM response at a 1.2 V assembly potential, following a different procedure in order to ensure that the gold oxide film was fully formed. In this case the electrode was first poised at 0.6 V and then poised at 0.9 V (vs. Ag/AgCl).

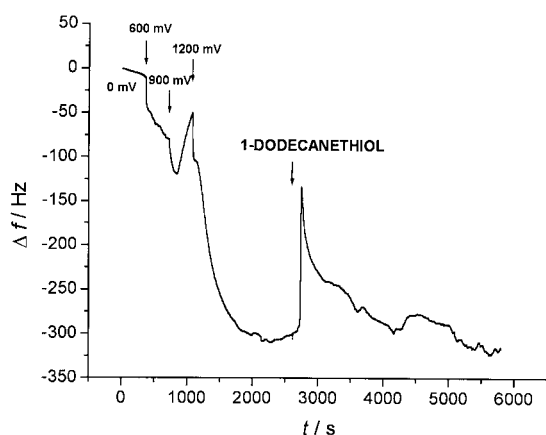


Fig. 9. Quartz crystal resonant frequency change after addition of 1-dodecanethiol to ethanolic 0.1 M NaClO<sub>4</sub> to final concentration of 1 mM at 1.2 V vs. Ag/AgCl; the gold was previously stepped from OCP to 600 and 900 mV successively as shown.

In all cases and at all potentials studied a decrease of resonant frequency was observed after addition of 1-dodecanethiol into the ethanol-based supporting electrolyte. In general there is an abrupt fall in the frequency on addition of 1-dodecanethiol followed by a slower variation, except for the crystal at open circuit potential.

Application of the Sauerbrey relationship [36] to the change of crystal resonant frequency and assuming that the frequency change can be related to mass change, an approximation discussed above, suggests that, for a close-packed 1-dodecanethiol monolayer (intermolecular spacing of 0.5 nm is considered) on a 10 MHz crystal, a 37 Hz decrease in frequency should be obtained. Correcting for surface roughness, a 40–50 Hz fall would be expected. Occasionally larger frequency changes were observed in repeat experiments. Since it is unlikely a monolayer of packing density larger than 0.78 nmol cm<sup>-2</sup> could be formed, a larger mass increase would have to occur in the form of a multilayer (this does not imply any form of organization or order) system [7].

Figure 8c at 0.6 V shows a much slower decline of frequency after ca. 700 s as most of the monolayer has assembled and high-rate mass increase has turned to a slow transformation process of ordering [30]. It can be seen that the rate of change of crystal resonant frequency due to adsorption at 0.6 V is clearly higher than that at OCP and at 0.0 V applied potential.

Concerning experiments at 1.2 V, addition of 1-dodecanethiol after 2600 s caused an abrupt frequency step upwards followed by exponential decay near to the value prior to addition. If alkanethiol adsorption to gold oxide was not possible and the gold surface was fully covered with oxide, no major change of frequency would have been observed. If the surface were not completely covered with oxide (most likely the case), at least partial monolayer assembly would take place accompanied by a frequency fall. The steep rise of resonant frequency after 1-dodecanethiol addition must therefore be a consequence of removal of the

oxide layer, and adsorption on unblocked gold surface in a slower process. The important deduction to be made from Figure 9 is that at 1.2 V the process is already much more complex and so that such positive potentials for SAM formation should be avoided at polycrystalline gold, although this was not evident from the other electrochemical characterization techniques employed.

#### 4. Conclusions

The application of positive potentials to gold surfaces during alkanethiol monolayer formation from dilute ethanolic solutions to improve the rate of alkanethiol adsorption has been investigated by various techniques. It was confirmed that the process of adsorption at controlled potentials is very fast and, as opposed to lengthy assembly at open circuit potential, well-packed 1-dodecanethiol monolayers are produced in such a way in time periods as short as 100 s. Adsorption of 1-dodecanethiol led to complete suppression of electron-transfer processes and a decrease of capacitive currents by an order of magnitude, indicative of defect-free, ordered and compact organic layers, under all conditions, including at potentials above that of gold oxide formation. The assembly of the monolayer essentially removed any roughness characteristics of the underlying substrate, which has been demonstrated for the first time to our knowledge.

It was shown that for these cases, the quartz crystal microbalance is an excellent tool for probing the rate of alkanethiol adsorption as a function of applied potential. The observed decreases in crystal resonant frequency imply full monolayers or even multilayer structures. It also showed, together with other techniques, that the best potential for fixed potential adsorption is 0.6 V, where any extra reactions from ethanol oxidation or reaction with gold oxide are not significant.

Further investigation of 1-dodecanethiol adsorption on fully-oxidized gold surfaces would be interesting, as well as investigating the role of water. This could be carried out by application of potentials above the potential of gold oxide formation in partially diluted ethanol (e.g. 80%) and subsequent addition of alkanethiol.

The studies undertaken here are important for the rapid formation of monolayers on gold substrates with a view to the fast construction of robust defect-free bilayers. It should be noted that these experiments were carried out at polycrystalline gold and not at the usual Au(111), which is therefore probably unnecessary as a bilayer substrate.

#### 5. Acknowledgements

Financial support from Fundação para a Ciência e Tecnologia (FCT), Portugal project POCTI (co-financed by the European Community fund FEDER), ICEMS (Research Unit 103), Slovak project VEGA 1/8310/01 and European Projects ERB-ICT15-CT960804 and QLK3-2000-01311, is gratefully acknowledged. S.K. thanks the European Phys-

ical Society for an exchange grant. We thank I. Novotny (Department of Microelectronics, Slovak University of Technology, Bratislava) for preparation of silicon plates with sputtered gold electrodes.

## 6. References

- [1] R. G. Nuzzo, D. L. Allara, *J. Am. Chem. Soc.* **1983**, *105*, 4481.
- [2] H. O. Finklea, *Electroanal. Chem.* **1996**, *19*, 109.
- [3] A. Ulman, *Chem. Rev.* **1996**, *96*, 1533.
- [4] C. E. D. Chidsey, C. R. Bertozzi, T. M. Putvinski, A. M. Mulscce, *J. Am. Chem. Soc.* **1990**, *112*, 4301.
- [5] S. Arnold, Z. Q. Feng, T. Kakiuchi, W. Knoll, K. Niki, *J. Electroanal. Chem.* **1997**, *438*, 91.
- [6] T. W. Schneider, D. A. Buttry, *J. Am. Chem. Soc.* **1993**, *115*, 12391.
- [7] Y. T. Kim, R. L. McCarley, A. J. Bard, *Langmuir* **1993**, *9*, 1941.
- [8] R. Elghanian, J. J. Storhoff, R. C. Mucic, R. L. Letsinger, C. A. Mirkin, *Science* **1997**, *277*, 1078.
- [9] Y. Feng, W. K. Teo, K. S. Siow, Z. Gao, K. L. Tan, A. K. Hsieh, *J. Electrochem. Soc.* **1997**, *144*, 55.
- [10] D. Mandler and I. Turyan, *Electroanalysis* **1996**, *3*, 207.
- [11] I. Turyan and D. Mandler, *Anal. Chem.* **1997**, *69*, 894.
- [12] N. A. Chaki, K. Vijayamohanam, *Biosens. Bioelectron.* **2002**, *17*, 1.
- [13] N. Nishimura, M. Ooi, K. Shimazu, H. Fujii, K. Uosaki, *J. Electroanal. Chem.* **1999**, *473*, 75.
- [14] A. Kumar, G. Whitesides, *Science* **1994**, *263*, 60.
- [15] K. Weber, L. Hockett, S. Creager, *J. Phys. Chem. B* **1997**, *101*, 8286.
- [16] R. Subramanian, V. Lakshminarayanan, *Electrochim. Acta* **2000**, *45*, 4501.
- [17] S. Lião, Y. Shnidman, A. Ulman, *J. Am. Chem. Soc.* **2000**, *122*, 3688.
- [18] C. Fruböse, K. Doblhofer, *J. Chem. Soc. Faraday Trans.* **1995**, *91*, 1949.
- [19] H. Ron, I. Rubinstein, *J. Am. Chem. Soc.* **1998**, *120*, 13444.
- [20] M. Dijkstra, B. Kamp, J. C. Hoogvliet, W. P. van Bennekom, *Langmuir* **2000**, *16*, 3852.
- [21] W. Paik, S. Eu, K. Lee, S. Chon, M. Kim, *Langmuir* **2000**, *16*, 10198.
- [22] C. A. Widrig, C. Chung, M. D. Porter, *J. Electroanal. Chem.* **1991**, *310*, 335.
- [23] T. Kawaguchi, H. Yasuda, K. Shimazu, M. D. Porter, *Langmuir* **2000**, *16*, 9830.
- [24] G. Tremiliosi-Filho, E. R. Gonzalez, A. J. Motheo, E. M. Belgsir, J.-M. Leger, C. Lamy, *J. Electroanal. Chem.* **1998**, *444*, 31.
- [25] S. Eu, W. Paik, *Chem. Lett.* **1998**, 305.
- [26] L. H. Dubois, R. G. Nuzzo, *Ann. Rev. Phys. Chem.* **1992**, *43*, 437.
- [27] D.-F. Yang, C. P. Wilde, M. Morin, *Langmuir* **1996**, *12*, 6570.
- [28] D.-F. Yang, M. Morin, *J. Electroanal. Chem.* **1998**, *441*, 173.
- [29] P. Diao, M. Guo, R. Tong, *J. Electroanal. Chem.* **2001**, *495*, 98.
- [30] L. V. Protsailo, W. R. Fawcett, *Electrochim. Acta* **2000**, *45*, 3497.
- [31] R. de Levie, *Electrochim. Acta* **1964**, *9*, 1231.
- [32] E. Boubour, R. B. Lennox, *Langmuir* **2000**, *16*, 4222.
- [33] A. Kowal, C. Gutierrez, *J. Electroanal. Chem.* **1995**, *395*, 243.
- [34] *CRC Handbook of Chemistry and Physics*, 64th ed., CRC Press, Boca Raton, Florida, **1983**.
- [35] D. A. Buttry, *Electroanal. Chem.* **1991**, *17*, 1.
- [36] G. Sauerbrey, *Z. Phys.* **1959**, *155*, 206.